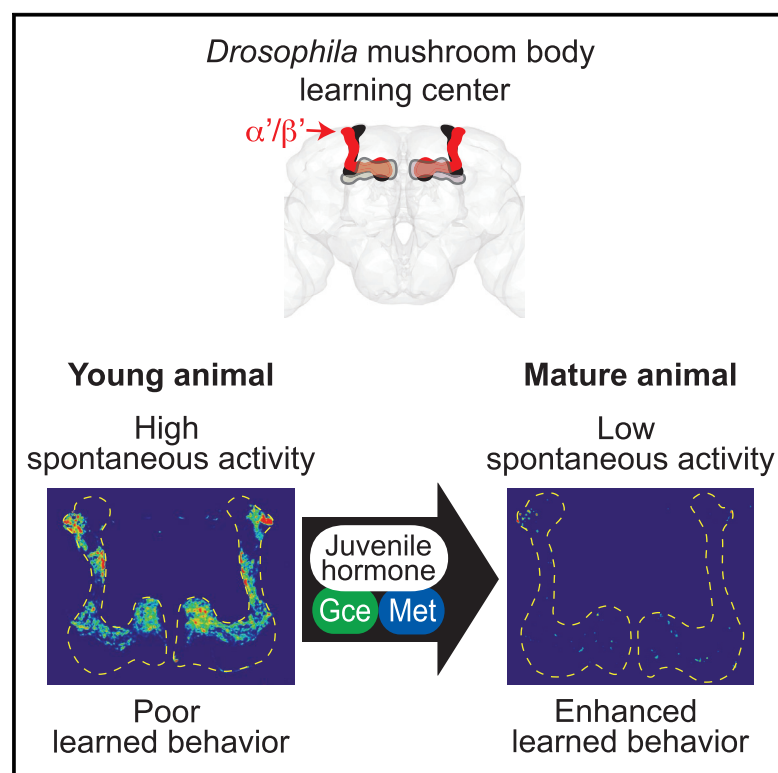


Juvenile hormone drives the maturation of spontaneous mushroom body neural activity and learned behavior

Graphical abstract



Authors

Sarah G. Leinwand, Kristin Scott

Correspondence

sleinwand@berkeley.edu (S.G.L.),
kscott@berkeley.edu (K.S.)

In brief

Leinwand and Scott discover that juvenile hormone signaling in an early sensitive period drives maturation of spontaneous neural activity in the *Drosophila* mushroom body learning center and coordinates enhancement of learned behavior. This work provides insight into age-dependent refinement of learning circuit activity and its essential function in learned behavior.

Highlights

- Spontaneous neural activity in a learning circuit decreases in early adulthood
- Cacophony voltage-gated calcium channels mediate the spontaneous activity
- Juvenile hormone signaling in an early sensitive period triggers activity maturation
- Hormone signaling in young animals is required for enhanced learned behavior

Article

Juvenile hormone drives the maturation of spontaneous mushroom body neural activity and learned behavior

Sarah G. Leinwand^{1,*} and Kristin Scott^{1,2,*}

¹Department of Molecular and Cell Biology and Helen Wills Neuroscience Institute, University of California, Berkeley, Berkeley, CA 94720, USA

²Lead contact

*Correspondence: sleinwand@berkeley.edu (S.G.L.), kscott@berkeley.edu (K.S.)

<https://doi.org/10.1016/j.neuron.2021.04.006>

SUMMARY

Mature behaviors emerge from neural circuits sculpted by genetic programs and spontaneous and evoked neural activity. However, how neural activity is refined to drive maturation of learned behavior remains poorly understood. Here, we explore how transient hormonal signaling coordinates a neural activity state transition and maturation of associative learning. We identify spontaneous, asynchronous activity in a *Drosophila* learning and memory brain region, the mushroom body. This activity declines significantly over the first week of adulthood. Moreover, this activity is generated cell-autonomously via Cacophony voltage-gated calcium channels in a single cell type, α'/β' Kenyon cells. Juvenile hormone, a crucial developmental regulator, acts transiently in α'/β' Kenyon cells during a young adult sensitive period to downregulate spontaneous activity and enable subsequent enhanced learning. Hormone signaling in young animals therefore controls a neural activity state transition and is required for improved associative learning, providing insight into the maturation of circuits and behavior.

INTRODUCTION

Genetic programs and experience in the form of neural activity refine neural circuits, sculpting cognitive function over time. Activity state transitions in neural circuits are widespread during normal development (Akin et al., 2019; Ben-Ari et al., 1989; Blankenship and Feller, 2010; Farooq and Dragoi, 2019; Piekarski et al., 2017). Achieving the mature activity state is correlated with the emergence of adult behavioral outputs (Farooq and Dragoi, 2019; Kirkby et al., 2013). For example, periodic waves of spontaneous neural activity occur throughout immature visual, somatosensory, and motor brain regions in perinatal critical periods, before distinct, less correlated sensory-evoked or locomotion-related activity patterns emerge in older animals (Blankenship and Feller, 2010). Periodic bursts of spontaneous activity also occur in the hippocampus, specifically in early mammalian post-natal development, in a brief period prior to development of robust long-term potentiation (Ben-Ari et al., 1989; Harris and Teyler, 1984). Although temporal evolution of spontaneous neural activity patterns is prevalent in developing circuits, the molecular mechanisms that control the timing of neural activity state transitions and coordinate maturation of behavioral outputs in young animals are largely unknown.

Hormones regulate multiple aspects of the maturation of the nervous system. Systemic hormonal signaling controls neural dif-

ferentiation, remodeling, physiology, and other key events for the refinement of neural circuits (Flatt et al., 2006; Joëls, 1997; Piekarski et al., 2017; Rivas and Naranjo, 2007). For example, sex steroid hormones act transient in a critical prenatal window to regulate the development of neural circuits for sexually dimorphic behaviors, producing enduring changes in the brain (Wu et al., 2009). Furthermore, many hormone receptors directly alter transcription and consequently have direct or indirect effects on ion channels, synapses, and neurotransmission (Alyagor et al., 2018; Morsink et al., 2006; Nunez et al., 2008; Piekarski et al., 2017). Gonadal hormone signaling accelerates the maturation of inhibitory neurotransmission in cortical circuits, with correlated effects on behavior (Piekarski et al., 2017). Moreover, thyroid hormones regulate synaptic transmission in the hippocampus in young animals (Rivas and Naranjo, 2007), with clear implications for memory. Juvenile hormone (JH) is an insect hormone with functional similarities to mammalian thyroid hormones (Flatt et al., 2006). JH circulates widely and acts on diverse neural circuits in young animals to regulate metamorphosis, reproduction, and courtship (Bilen et al., 2013; Lin et al., 2016). Across species, hormonal signaling is therefore well poised to coordinate key transitions in the maturation of the nervous system and behavior at particular stages of animal development.

A mechanistic understanding of how the nervous system achieves activity state transitions will provide insight into the

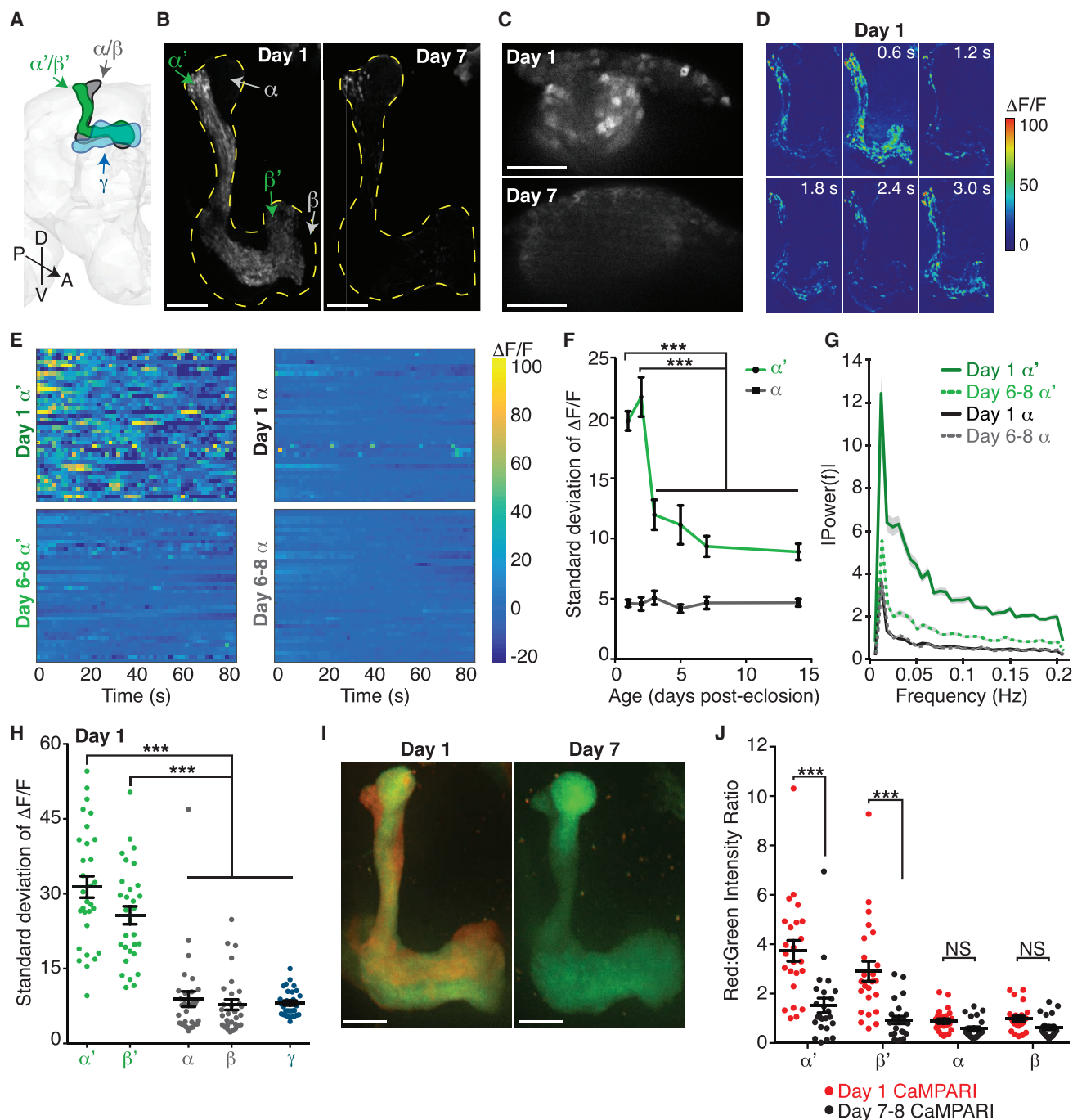


Figure 1. Age-dependent decrease in α'/β' KC neural activity

(A) Schematic illustration of the three subtypes of Kenyon cells (KCs) in the mushroom body (MB) in one hemisphere of the fly central brain: γ (blue), α'/β' (green), and α/β (gray). MB lobes are composed of spatially distinct axonal projections of the three KC subtypes (colored regions), while MB calyx with KC somas and dendrites is located posterior to the MB lobes. Brain orientation as indicated: A, anterior; D, dorsal; P, posterior; V, ventral.

(B and C) Representative standard deviation projection images reveal MB lobes (outlined by yellow dotted lines) or calyx regions with most variability in GCaMP6s signal, indicating high activity levels in day 1 α'/β' KCs and lower activity levels in day 7 α'/β' KCs and in α/β and γ KCs of both ages. Individual α'/β' and α/β KCs all have bifurcating axons, with one branch projecting in the vertical α' or α lobe and one branch projecting in the horizontal β' or β lobe.

(D) Sequence of representative, pseudo-colored $\Delta F/F$ images of the change in GCaMP activity over time, at 0.6-s intervals, in day 1 KCs.

(E) Heatmaps of $\Delta F/F$ of GCaMP activity in α' and α regions of interest (ROIs) of day 1 (top) or days 6–8 (bottom) KCs over time with warmest colors representing the largest changes in activity from the average over the entire recording. Rows in heatmap are representative ROIs, each from a different fly (40 flies).

(legend continued on next page)

origins of mature behaviors. Critically, evaluating the role of hormones in neural activity and behavior maturation requires isolating their effects on specific cells in known circuits and at particular developmental times. The fruit fly *Drosophila melanogaster* system offers powerful genetic tools to causally link *in vivo* neural activity with behavior and to manipulate gene expression, with single-cell resolution. Recently, high levels of spontaneous neural activity were observed in the developing *Drosophila* visual system (Akin et al., 2019; Akin and Zipursky, 2020), illustrating that activity maturation occurs in invertebrate systems, as well as vertebrates. In examining activity in the adult fly brain, we observed high levels of activity in the *Drosophila* mushroom body (MB) brain region that declined rapidly with age. The MB is critical for learned behavior (Dubnau et al., 2001; McGuire et al., 2001). Physiological, molecular, behavioral, and anatomical studies, including a complete connectome, have provided a uniquely rich understanding of the neuronal architecture and function of the MB (Aso et al., 2014; Inada et al., 2017; Krashes et al., 2007; Lee et al., 1999; Takemura et al., 2017; Turner et al., 2008). Our discovery of an immature to mature activity state transition in this well-described system offers an entry point to rigorously examine how neural activity in young animals drives refinement and maturation of behavior.

Here, we employ *in vivo* functional imaging and powerful genetic tools to describe a high spontaneous activity state in the *Drosophila* MB learning and memory brain center of young animals and its crucial role in the maturation of learned behavior. We identify spontaneous, asynchronous activity specifically in one MB cell type, the α'/β' Kenyon cells (KCs), in young animals, which unexpectedly declines over the first week of adulthood. We find that Cacophony (Cac) voltage-gated calcium channels mediate this young animal spontaneous activity. We report that JH, a crucial regulator of insect development similar to vertebrate thyroid hormones, signaling specifically in α'/β' KCs during a sensitive period in early adulthood coordinates the maturation of neural activity states and is required for mature associative learning.

RESULTS

Neural activity in a learning and memory brain center decreases over the first week of adulthood

While examining calcium activity in the *Drosophila* brain, we observed fluctuating baseline activity in the MB learning and

memory brain region. The principal intrinsic MB cells are the KCs (Figure 1A). The approximately 2,000 KCs are critical for integrating information about conditioned and unconditioned stimuli to form learned associations (Aso et al., 2014; Krashes et al., 2007). To further investigate the observed activity, we performed *in vivo* calcium imaging of all KCs in adult flies of different ages. We observed frequent fluctuations in GCaMP6 calcium activity in KC axons (Figures 1B, 1D, and 1E; Video S1) and dendritic claw and soma regions (Figures 1C and S1A) in young adults, from eclosion (on day 0) through day 2, without stimulation. This activity was prominent in a spatially restricted portion of the MB, the α'/β' lobe (Figures 1A, 1B, and 1D–1F), showing high variance in the GCaMP6s signal (Figures 1E and 1F), with an average frequency of 0.0584 ± 0.0032 Hz and no underlying periodicity or synchronicity (Figures 1G and S1B). Unexpectedly, we found that the frequency and amplitude of KC activity declined significantly with age; activity decreased by the third day of adulthood and remained at stable, lower levels in more mature flies, from days 6–8 through days 13–15 (average α'/β' frequency at days 6–8 is 0.0339 ± 0.0031 Hz; Figures 1B–1G and S1B; Video S2). The large decrease in KC activity from day 1 (hereafter referred to as young) to days 6–8 (hereafter referred to as mature) occurred in both males and females (Figures S1C and S1D). The age-dependent decrease, kinetics, and asynchronous nature of this activity are distinct from previously reported pupal and adult MB activity patterns (Jiang et al., 2005; Rosay et al., 2001). Thus, we discovered a switch from a high-activity state, composed of asynchronous, unpatterned activity, to a low-activity state in the KC learning circuit in the first week of adulthood.

The MB is composed of three functionally distinct KC subtypes that develop sequentially: γ (born in third instar larva; required for short-term memory), α'/β' (late larva; memory acquisition and consolidation), and α/β (pupae; memory retrieval), with spatially segregated axonal projections in the MB lobes (Figure 1A) (Dubnau et al., 2001; Krashes et al., 2007; Lee et al., 1999; Pascual and Pr  at, 2001). Our functional imaging suggested that young adult activity primarily localized to α'/β' KCs (Figures 1B and 1D–1G). Using KC subtype-specific drivers, we confirmed frequent, asynchronous calcium transients in the α'/β' KCs of young flies (Figure 1H). Young α/β KCs displayed only rare calcium transients, and young γ KC activity was nearly undetectable (Figure 1H). Thus, age-dependent regulation of

(F) Standard deviation of $\Delta F/F$ reflects baseline activity levels in ROIs containing α' (green) or α (black) KCs at different ages from day 1 to 14. Points are averages of 30–44 flies. *** $p < 0.001$, two-way ANOVA with significant lobe and age effects and Sidak's multiple comparisons test. Additionally, α' and α are significantly different at each age ($p < 0.001$), whereas all α activity is not significantly different across the age groups.

(G) Fourier transform analysis of the baseline neural activity in ROIs containing α' or α KCs of day 1 or day 6–8 flies. Activity from 40 flies per age was used for analysis.

(H) Standard deviation of $\Delta F/F$ reflects baseline activity levels for day 1 KCs imaged using KC-subtype-specific drivers (γ , α'/β' , and α/β). Individual α'/β' and α/β KC axons bifurcate, with one branch in the vertical α' or α lobe and one branch in the horizontal β' or β lobe. Each dot represents median ROI from one fly (α' and β' ROIs and α and β ROIs are from anatomically distinct regions within the same flies). $n = 15$ flies with each hemisphere of the brain shown as one point. *** $p < 0.001$, one-way ANOVA with Tukey's multiple comparisons test.

(I) Representative images of photoconverted CaMPARI expressing KCs at day 1 or 7, with red fluorescence indicating high activity at time of *in vivo* UV stimulus presentation.

(J) Red-to-green intensity ratio quantification of CaMPARI signal in large ROIs drawn from α' , β' , α , and β lobes of day 1 (red dots) or day 7–8 (black dots) flies. $n = 12$ flies with each hemisphere of the brain shown as one point. *** $p < 0.001$, two-way ANOVA with significant lobe and age effects and Sidak's multiple comparisons test.

(B–J) Ages in days post-eclosion (day 0). White scale bars are 20 μ m. Error bars are mean and SEM. See also Figure S1.

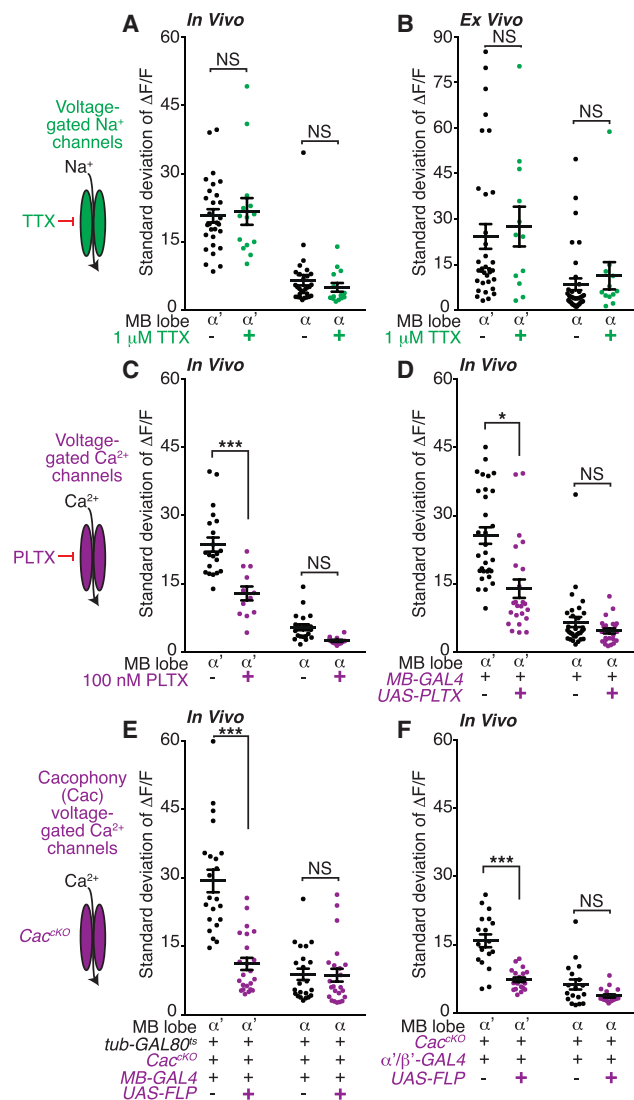


Figure 2. Cac voltage-gated calcium channels mediate spontaneous α'/β' KC activity

(A and B) KC GCaMP activity with or without acute tetrodotoxin (TTX; 1 μM beginning 10 min prior to assay) treatment to block voltage-gated sodium channels (A) *in vivo* or (B) *ex vivo*. $n = 6$ –16 flies.

(C) *In vivo* KC activity with acute perfusion of the voltage-gated calcium channel antagonist Plectroreus toxin (PLTX; 100 nM). $n = 6$ –10 flies.

(D) *In vivo* activity of KCs expressing genetically encoded, membrane-tethered PLTX peptides. $n = 12$ –15 flies.

(E) *In vivo* activity of *Cacophony* (Cac) conditional knockout KCs. Mutation induced by shifting flies to 30°C at late pupal stage to remove *tub-GAL80^{ts}* repression of the KC-expressed FLP enzyme. $n = 11$ flies.

(F) *In vivo* activity of α'/β' -specific Cac conditional knockout KCs. $n = 9$ –10 flies. Activity is recorded from flies expressing LexAop-GCaMP6s under the pan-KC driver MB247-lexA.

(A–F) Day 1 flies imaged. Each point is median ROI for the indicated lobe, with each hemisphere of the brain of a fly shown as one point. Flies express UAS-GCaMP6s in all KCs except as noted in (F). Error bars are mean and SEM. $^{NS}p > 0.05$; $^{***}p < 0.001$; $^{*}p < 0.05$, two-way ANOVA with Sidak's multiple comparisons test. All comparisons for α lobe are not significant (NS). See also Figure S2.

activity does not reflect cell maturation based on KC birth order (Lee et al., 1999).

To independently assess the age-dependent decrease in α'/β' KC activity, we used the genetically encoded, ratiometric calcium integrator CaMPARI, which photoconverts from green to red in the presence of high intracellular calcium and UV illumination (Fosque et al., 2015). *In vivo* application of a brief UV stimulus (5 s) to CaMPARI-expressing KCs revealed significantly higher activity in the α'/β' KCs of young flies than of mature flies (Figures 1I and 1J). Consistent with our GCaMP imaging, no age-dependent CaMPARI changes were observed in α/β (Figures 1I and 1J). These data demonstrate learning circuit maturation: a specific decrease in α'/β' KC activity over the first week of adulthood.

α'/β' KC activity is spontaneous and mediated by voltage-gated calcium channels

We investigated whether the KC activity in young animals is generated spontaneously or driven by sensorimotor inputs. Three lines of evidence argue that the activity is spontaneously and cell-autonomously generated. First, we severed all sensorimotor inputs to the brain to test whether they contribute to α'/β' KC activity. We found that α'/β' KC activity persisted in *ex vivo* explant brains (Figures 2A and 2B), indicating that this activity is not evoked by sensorimotor cues. Second, we perfused tetrodotoxin (TTX) to block the voltage-gated sodium channels that drive action potentials (Zhang and Gaudry, 2018). We used a concentration of TTX that effectively inhibits synaptic transmission in similar preparations (Rosay et al., 2001; Tuthill and Wilson, 2016; Zhang and Gaudry, 2018; Zhou et al., 2019). However, TTX had no effect on α'/β' KC activity *in vivo* and *ex vivo*, suggesting that circuit inputs are dispensable for this activity (Figures 2A and 2B). Third, we tested whether gap junctions contribute to the activity. However, pharmacological blockade of gap junctions with 2-octanol (Liu et al., 2016) and RNAi knockdown of gap junction forming innexin subunits had no effect on α'/β' KC activity (Figure S2A and data not shown). This evidence that gap junctions do not contribute is consistent with the asynchronous nature of the activity across the KC population. Together, these results demonstrate that α'/β' KCs spontaneously and cell-autonomously generate calcium activity in young adults.

Because voltage-gated sodium channels are dispensable, we next examined whether the calcium activity was due to extracellular calcium influx or calcium release from internal stores. Pre-incubation of young adult brains with the cell-impermeant calcium chelator EGTA significantly reduced *in vivo* α'/β' KC spontaneous activity (Figure S2B), indicating that extracellular calcium is required for spontaneous activity. Moreover, both pharmacology and RNAi knockdown experiments indicate that calcium release from internal stores is unlikely to contribute. Specifically, acute application of thapsigargin, an irreversible inhibitor of the SERCA calcium-ATPase pump in the endoplasmic reticulum that is required for calcium release from internal stores (Murmur et al., 2010), had no effect on α'/β' KC spontaneous activity (Figure S2C). Similarly, RNAi-mediated knockdown of genes involved in intracellular calcium release, the *inositol 1,4,5-tris-phosphate receptor* (*Itpr*), the *ryanodine receptor*

(*RyR*) (Xu et al., 2017; Yamanaka et al., 2015), and *SERCA*, had no effect on α'/β' KC spontaneous activity (Figures S2D and S2E).

Consequently, we hypothesized that voltage-gated calcium channels participate. Hyperpolarizing KCs with the green-light-gated anion channel *gtACR1* (Mohammad et al., 2017) was sufficient to block all young adult α'/β' KC spontaneous activity (Figure S2B), consistent with the involvement of a voltage-gated channel. We therefore probed calcium channels directly, using plecteurys toxin (PLTX) to irreversibly inhibit voltage-gated calcium channels (Gu et al., 2009). Acute PLTX treatment significantly reduced α'/β' KC spontaneous activity in young flies (Figure 2C), consistent with previous studies examining activity in dissociated, cultured KCs (Jiang et al., 2005). KC-specific expression of a genetically encoded, membrane-tethered PLTX peptide (Choi et al., 2014) also significantly reduced α'/β' KC spontaneous activity (Figure 2D), further demonstrating that voltage-gated calcium channels mediate the spontaneous α'/β' KC activity.

Prior research suggests that PLTX may antagonize *Cac* voltage-gated calcium channels (Gu et al., 2009). Moreover, α'/β' KCs express the voltage-gated calcium channels *Cac*, *Ca- α 1D*, and *Ca- β* (Croset et al., 2018; Davie et al., 2018). We performed RNAi knockdown experiments to test whether these channels contribute to α'/β' KC spontaneous activity. RNAi knockdown of *Cac* channels significantly reduced young adult α'/β' KC activity, whereas RNAi against *Ca- α 1D* or *Ca- β* had no or mixed effects (Figure S2F). We also generated a KC-specific *Cac* conditional null mutant (Fisher et al., 2017) in which the mutation was induced in late pupae, approximately 24 h prior to eclosion, thereby minimizing early developmental defects and compensatory mechanisms. These *Cac*^{CKO} mutants exhibited a significant reduction in α'/β' KC spontaneous activity (Figure 2E). Importantly, restriction of *Cac*^{CKO} to only the normally highly active α'/β' KCs was sufficient to significantly reduce α'/β' KC spontaneous activity levels (Figure 2F). Together, these results demonstrate that young α'/β' KCs generate spontaneous calcium activity mediated by *Cac* voltage-gated calcium channels, and this activity decreases as the animal matures.

JH signaling sculpts α'/β' KC activity maturation

What underlying molecular mechanisms orchestrate the age-dependent decrease in α'/β' KC spontaneous activity? Ecdysone and JH are essential hormonal modulators of early development and behavioral maturation (Argue et al., 2013; Bilen et al., 2013; Jindra et al., 2013; Lin et al., 2016; Marchetti and Tavano, 2017; Zhang et al., 2019); therefore, we hypothesized that they might serve as systemic signals that modulate KC activity with age. We found that ecdysone is dispensable for KC activity maturation, as decreasing ecdysone levels systemically (Gaziová et al., 2004) or decreasing candidate MB-expressed ecdysone receptors (Lark et al., 2017; Lee et al., 2000) specifically in KCs did not influence spontaneous activity in young or mature animals (Figures S3A–S3C). We next tested JH, which is secreted into the hemolymph where it may circulate widely, like mammalian thyroid hormones (Bilen et al., 2013; Jindra et al., 2013). We fed flies precocene, which induces specific cytotoxicity to kill JH-producing cells beginning at eclosion

(Argue et al., 2013; Lin et al., 2016). Precocene consumption resulted in mature flies that retained abnormally high, young-like levels of spontaneous α'/β' KC activity (Figure S3D). This suggests that JH normally drives the age-dependent decrease in α'/β' KC spontaneous activity.

JH signals via two hormone receptors, Methoprene-tolerant (*Met*) and Germ cell expressed (*Gce*), which are basic helix-loop-helix Per-Arnt-Sim transcriptional regulators (Jindra et al., 2015; Miura et al., 2005). *Met* and *Gce* are strongly expressed throughout the MB (Baumann et al., 2017). We found that when both *Met* and *Gce* were knocked down specifically in α'/β' KCs, the age-dependent activity decrease was blocked: mature receptor knockdown flies displayed high levels of α'/β' KC spontaneous activity similar to young flies, as measured by GCaMP6s calcium imaging (Figures 3A, 3B, and S3E) and CaM-PARI photoconversion (Figures 3C and 3D). This hormone effect on activity is specific to mature animals, because activity was similar between knockdown and genetic controls in young flies (Figures 3B and 3D). Flies expressing RNAi against *Met* or *Gce* individually in α'/β' KCs, as well as hypomorphic *Met*¹ mutants (Wilson and Fabian, 1986), also displayed high levels of α'/β' KC spontaneous activity in both young and mature animals (Figures S3F–S3H). Together, these results demonstrate that JH signals through *Met* and *Gce* expressed in α'/β' KCs to decrease spontaneous activity over the first week of adulthood.

We next examined the nature of the high activity retained upon manipulation of hormonal signaling and found that it recapitulated essential features of the young activity state. Notably, *ex vivo* imaging of dissected brains revealed similarly high levels of α'/β' KC activity in both young and mature brains with *Met* and *Gce* knocked down specifically in α'/β' KCs (Figure S3I), demonstrating sensorimotor-independent spontaneous activity similar to young wild-type animals (Figure 2B). Additionally, acute *in vivo* inhibition of voltage-gated calcium channels with PLTX treatment greatly reduced the spontaneous activity in both young and mature flies with *Met* and *Gce* knocked down (Figure S3J), indicating that the activity is indeed mediated by the same channels as young wild-type activity (Figure 2C). Thus, blocking JH signaling extends the high α'/β' KC spontaneous activity normally present in young animals, arguing that JH is the master regulator required to transition from the young to the mature activity state.

JH titer is maximal around the time that adult flies eclose and then falls rapidly within the first 72 h of adulthood (Bownes and Rembold, 1987; Zhang et al., 2019), a time course similar to the observed decrease in α'/β' KC activity (Figure 1F). To gain insight into the developmental time window in which JH signaling exerts its effects on KC spontaneous activity, we restricted the knockdown of *Met* and *Gce* in KCs to an early post-eclosion period (day 0–2) or a period late in the first week of adulthood (day 4–7) with the temperature sensitive repressor *tub-GAL80^{ts}* (McGuire et al., 2003). Mature day 7 animals with *Met* and *Gce* knocked down only from day 0 to 2 displayed aberrantly high α'/β' KC spontaneous activity (Figures 3E and 3F). In contrast, knockdown of *Met* and *Gce* later in adulthood, from day 4 to 7, did not influence the maturation of α'/β' spontaneous activity (Figures 3E and 3F). Together, these experiments show that JH acts in an early sensitive period circa eclosion (day 0–2) to drive

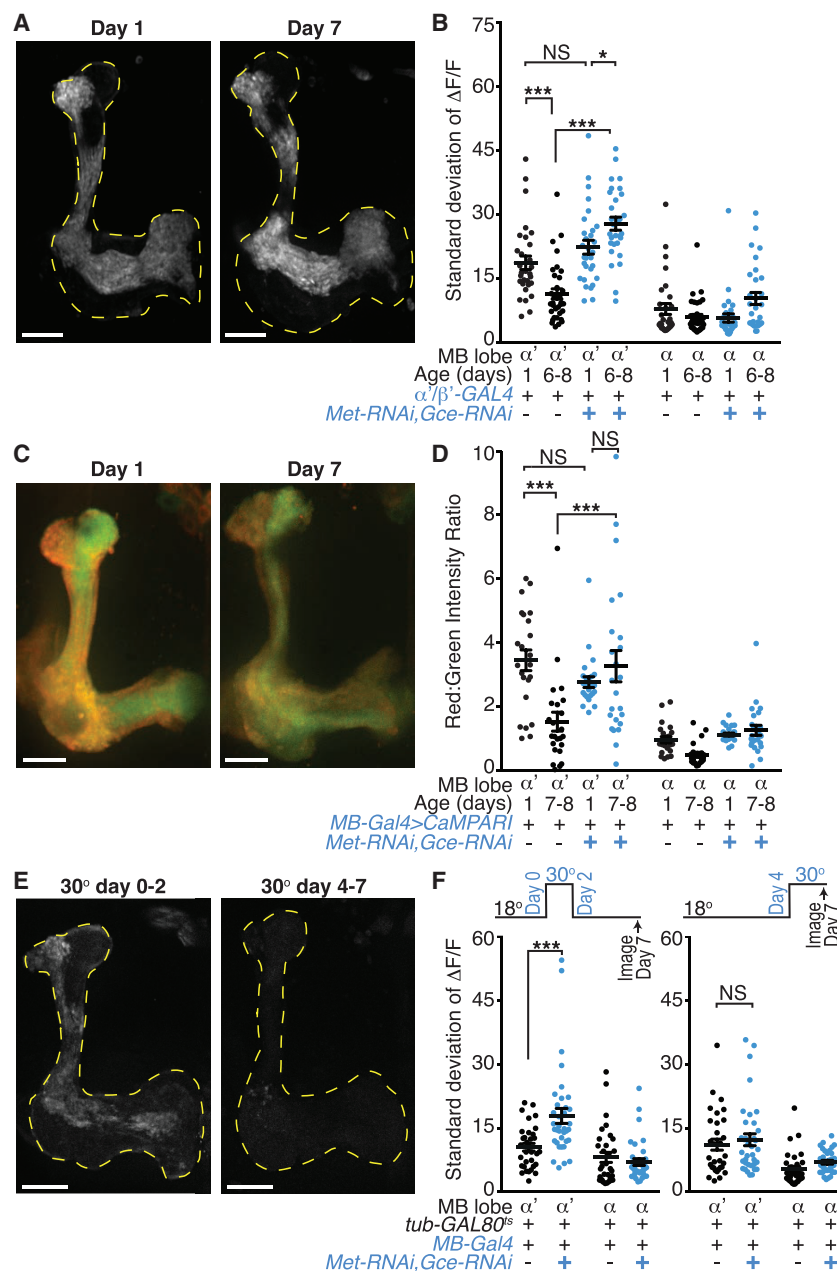


Figure 3. Juvenile hormone (JH) signaling via Met and Gce downregulates spontaneous α'/β' activity

(A) Representative standard deviation projection images of flies with α'/β' expression of *Met* and *Gce* RNAi transgenes show MB lobe (yellow dotted lines) regions with high GCaMP6s activity at day 1 or 7.

(B) KC activity in genetic controls and in flies with α'/β' expression of *Met* and *Gce* RNAi transgenes at day 1 or 6–8. $n = 15$ –17 flies with each hemisphere of the brain shown as one point.

(C) Representative images of photoconverted CaMPARI in *Met* and *Gce* RNAi expressing KCs at day 1 or 7. Red fluorescence indicates high activity at time of *in vivo* UV stimulus presentation.

(D) Red-to-green intensity ratio quantification of CaMPARI signal in large ROIs drawn from α' and α lobes of genetic controls or flies with KC expression of *Met* and *Gce* RNAi at day 1 or 7–8. $n = 12$ flies with each hemisphere of the brain shown as one point.

(E) Representative standard deviation projection images of day 7 flies with KC-specific *Met* and *Gce* knockdown temporally restricted (by the repressor *tub-GAL80^{ts}* and a shift to 30°C) to the immediate post-eclosion period (days 0–2) or to later in adulthood (days 4–7).

(F) KC activity in genetic controls and in flies with KC expression of *Met* and *Gce* RNAi transgenes temporally restricted by the repressor *tub-GAL80^{ts}*. Flies were shifted from 18°C to 30°C to induce the RNAi from either (left graph) eclosion until day 2, then returned to 18°C until imaging as mature day 7 animals, or (right graph) day 4 until immediately prior to imaging on day 7. $n = 16$ –18 flies with each hemisphere of the brain shown as one point.

(A, C, and E) White scale bars are 20 μm . (B and F) Each point is activity in median ROI for indicated lobe. (B, D, and F) Error bars are mean and SEM. NS, $p > 0.05$; *** $p < 0.001$; * $p < 0.05$, two-way ANOVA with Sidak's multiple comparisons test. All comparisons for α lobe are NS. See also Figure S3.

Mature learned behavior requires α'/β' KC activity and JH signaling in early adulthood

KCs are critical for sequential stages of associative learning and memory, with α'/β' KCs primarily contributing to memory

a maturation process that normally reduces α'/β' KC spontaneous activity. Thus, JH may exert an early organizational effect on the MB circuit.

We also examined whether JH signaling is a limiting factor for activity maturation. However, feeding flies a JH analog, Methoprene, to increase the hormone titer (Lin et al., 2016), or overexpressing *Met* (Bischof et al., 2013) receptors in KCs had no effect on young or mature flies' spontaneous KC activity (data not shown; Figure S3K). These experiments suggest that circulating JH may already be saturating, or alternatively, high spontaneous activity in young animals represents the default state, and additional JH action cannot precociously drive circuit maturation.

acquisition and consolidation (Aso et al., 2014; Dubnau et al., 2001; Krashes et al., 2007; Masek et al., 2015). Therefore, we hypothesized that α'/β' KC spontaneous activity and its maturation contribute to learned associations. For example, high activity in young animals might represent a critical period when learning is enhanced or might reflect an immature circuit not yet capable of forming robust associations. To distinguish these possibilities, we examined whether the ability to learn associations changes with age. We used an aversive taste memory task in which sucrose gustatory detection on the legs is briefly paired with bitter gustatory detection on the proboscis (Figure 4A) (Kirkhart and Scott, 2015; Masek et al., 2015; Masek and Scott, 2010). Flies

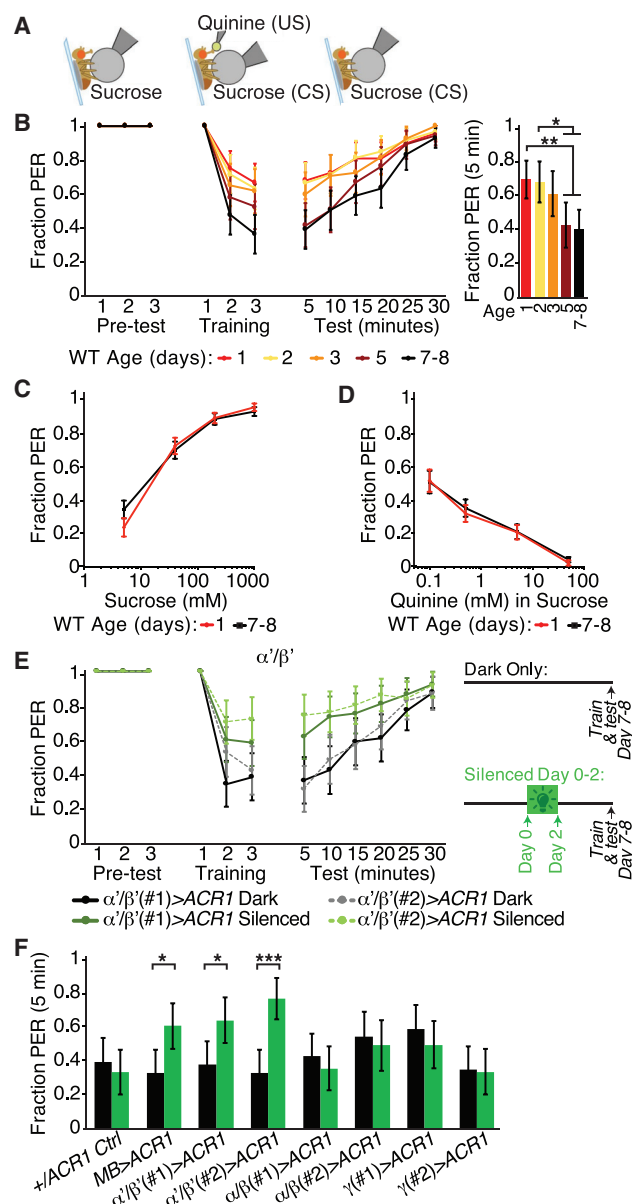


Figure 4. α'/β' KC activity in early adulthood is required for mature aversive taste memory behavior

(A) Schematic of aversive taste memory behavioral assay. Flies were presented with 200 mM sucrose three times (pre-test), and only flies that showed reliable PER were included for the remainder of the experiment. Next, flies were presented with sucrose on their legs, and their proboscis was touched with bitter 50 mM quinine upon PER (training pairing) three times. Finally, flies were presented with sucrose to the legs at 5-min intervals post-training to test learning. Learned behavior is independent of post-ingestive feedback.

(B) Aversive taste memory of wild-type CantonS flies of different ages, with bar graph representing data from the first 5-min test period.

(C) Innate responses to sucrose (5, 40, 200, 1,000 mM) presented three times each to the legs at day 1 or 7–8.

(D) Innate responses to bitter (0.1, 0.5, 5, and 50 mM quinine mixed with 100 mM sucrose) presented three times each to the proboscis at day 1 or 7–8.

(E) Aversive taste memory of mature day 7–8 flies; comparison of sibling controls reared in the dark only (no silencing, black or gray lines) and flies

learn from these pairings to avoid extending their proboscis to sucrose alone (Figure 4A). Previous studies demonstrated that γ and α'/β' KCs are essential for aversive taste memory (results replicated in Figure S4A) (Kirkhart and Scott, 2015; Masek et al., 2015).

We examined aversive taste memory throughout the first week post-eclosion and observed that learning performance increased with age (Figure 4B). Young flies showed significantly decreased learned aversion, with higher proboscis extension response (PER) to the sucrose conditioned stimulus after aversive pairing than mature flies (Figure 4B). The failure of young flies to learn the association was apparent after the first pairing of sugar and bitter and persisted for many minutes during the testing phase, representing a deficit in acquisition and perhaps also retention. Critically, the altered performance of young flies was not due to age-dependent changes in innate PER to sugar or bitter taste alone (Figures 4C and 4D). Thus, associative learning matures and improves in early adulthood, consistent with a model that the MB becomes competent to form robust associations in early adulthood and that the high spontaneous activity in young animals represents an immature state.

Is high α'/β' KC activity in young animals an essential step in the maturation of circuits for learned behavior? To examine this, we hyperpolarized KC subsets with the green-light-gated anion channel gtACR1 (Mohammad et al., 2017) exclusively beginning circa eclosion and for the first 2 days of adulthood, because gtACR1 acutely blocked KC spontaneous activity (Figure S2B). We then probed aversive taste memory behavior in these animals at days 7–8, under conditions that do not activate gtACR1. Hyperpolarizing α'/β' KCs exclusively from day 0 to 2 significantly impaired learning in mature animals (Figures 4E and 4F). In contrast, hyperpolarizing α'/β' KCs from day 4 to 7 did not impact mature learned behavior (Figure S4B). Hyperpolarizing all KCs from day 0 to 2 also impaired subsequent mature animal learning, whereas silencing only α/β or γ KCs from day 0 to 2 did not impair subsequent mature learning (Figures 4F and S4C–S4E). Importantly, this light exposure alone did not impact behavioral performance in genetic control animals (Figures 4F and S4C), and gtACR1-mediated silencing of KCs in early adulthood did not produce gross morphological abnormalities (Figure S4F). This demonstrates that the presence of high α'/β' KC activity during early adulthood is critical for establishing the circuits for subsequent learning in mature animals.

Because JH signaling is a key regulator of the maturation of α'/β' KC spontaneous activity, we hypothesized that JH coordinates the observed maturation of learned behavior. Indeed,

reared in green light from eclosion to day 2 to induce early adult developmental silencing of α'/β' with gtACR1 (two independent drivers, green lines).

(F) Aversive taste memory of mature day 7–8 flies at 5-min test period for dark-reared sibling controls (black bars) and flies reared in green light from eclosion to day 2 to induce early adult developmental silencing of no, all, or subtypes of KCs with gtACR1 (green bars). Two independent genetic drivers used for each KC subtype.

(B, E, and F) $n = 46$ –71 flies. Data are shown as mean with 95% confidence interval error bars. *** $p < 0.001$; ** $p < 0.01$; * $p < 0.05$, Fisher's exact test with Benjamini-Hochberg false discovery rate adjustment. (C and D) $N = 52$ flies, data are shown as mean with SEM error bars; NS $p > 0.05$, Mann-Whitney U test with Bonferroni correction for multiple comparisons. See also Figure S4.

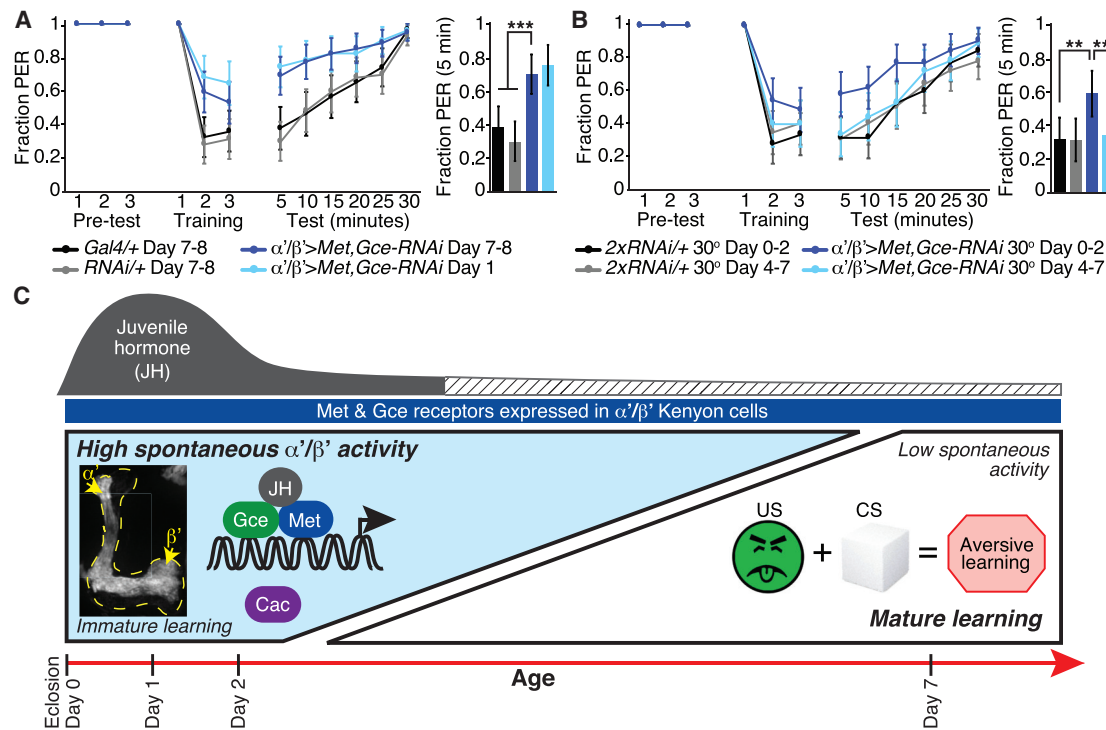


Figure 5. JH signaling in α'/β' KCs is required during a young animal sensitive period for mature aversive taste memory behavior

(A) Aversive taste memory of day 1 (light blue line) and day 7–8 flies (dark blue line) with *Met* and *Gce* knocked down in α'/β' KCs and of the day 7–8 genetic controls (black and gray lines).

(B) Aversive taste memory of mature day 7–8 flies. Comparison of flies with *Met* and *Gce* knocked down in α'/β' KCs only from day 0–2 (dark blue) or day 4–7 (light blue), when *tub-GAL80^{ts}* repression is removed by shifting the flies to 30°C, and temperature-matched genetic controls.

(C) Model for JH signaling via *Met* and *Gce* receptors expressed in α'/β' KCs from approximately eclosion to day 2 to drive a decrease in α'/β' spontaneous neural activity and maturation of learned behavior, in particular aversive taste memory, by day 7 of adulthood. Representative standard deviation projection image shows high spontaneous activity in day 1 α'/β' KCs. Spontaneous activity is mediated by *Cacophony* (*Cac*) voltage-gated calcium channels, and we hypothesize that *Cac* function may be indirectly downregulated with age by factors downstream of JH signaling that contribute to the excitability of α'/β' KCs.

(A and B) Bar graph represents data from the first 5-min test period. $n = 47$ –62 flies. Data are shown as mean with 95% confidence interval error bars. *** $p < 0.001$; ** $p < 0.01$, Fisher's exact test with Benjamini-Hochberg false discovery rate adjustment.

α'/β' -specific RNAi knockdown of the JH receptors *Met* and *Gce* impaired the aversive taste memory performance of mature flies compared with genetic controls (Figure 5A). Moreover, the learning performance of mature *Met* and *Gce* knockdown flies was as poor as their young counterparts (Figure 5A), indicating that age-dependent behavioral maturation was blocked. JH manipulation specifically impacted the mature behavior, because young *Met* and *Gce* knockdown flies performed like young wild-type flies (Figures 4B and 5A). Thus, JH normally drives the improvement in learning over the first week of adulthood. To examine when JH signaling is essential for the maturation of learning, we temporally restricted *Met* and *Gce* knockdown with *tub-GAL80^{ts}* and examined learned behavior at day 7. Disrupting JH signaling only from day 0 to 2, but not from day 4 to 7, impaired subsequent learned behavior in mature day 7 animals (Figure 5B). Thus, disrupting JH signaling specifically in α'/β' KCs in young animals elicits immature high α'/β' KC spontaneous activity and poor learned behavior in older animals, arguing that aberrant retention of the immature, high-activity state disrupts mature learning. Our findings are consistent

with a model in which JH, circulating at high levels in a sensitive period in very early adulthood, signals through *Met* and *Gce* receptors in α'/β' KCs to initiate a circuit maturation program that downregulates α'/β' KC spontaneous activity and coordinately improves mature learned behavior (Figure 5C).

DISCUSSION

Here, we show that JH acts on the α'/β' KCs of young adults to downregulate spontaneous activity and enhance associative learning in older animals. Specifically, we find that α'/β' KCs exhibit sensorimotor-independent, TTX-insensitive asynchronous activity in young animals that is mediated by *Cacophony* (*Cac*) voltage-gated calcium channels. JH signaling in a young animal sensitive period, when the titer of JH circulating is high (Bownes and Reibold, 1987; Zhang et al., 2019), is required to achieve the mature, low KC activity state and enhance learned behavior. Our discovery that a hormone triggers a neural activity state transition essential for robust learning provides a model for mechanistically probing the maturation of learning circuits and behavior.

Many animals are born with immature learning capabilities. In mammals, periodic giant depolarizing potentials occur in the immature hippocampus (Ben-Ari et al., 1989). Because multiple hippocampus-dependent learned behaviors are poor at the time of the giant depolarizing potentials and mature slowly over the first post-natal month (Ben-Ari et al., 1989; Farooq and Dragoi, 2019; Foster and Burman, 2010), a correlation between this pattern of spontaneous activity and learning is apparent. However, causal links between hippocampal activity patterns and maturation of learned behavioral outputs are lacking, despite their profound implications for the plasticity to form new associations throughout adulthood. Our studies demonstrate that *Drosophila* associative learning improves over the first week of adulthood and that appropriately regulated activity state transitions in higher-order brain regions are necessary for this learning maturation.

Our studies reveal that the spontaneous activity generated in young α'/β' KCs is critical for honing the neural circuits that subsequently produce mature learning. Notably, the activity in young KCs is asynchronous and unpatterned, unlike the propagating waves of activity in immature visual and somatosensory areas or the rhythmic alternations in motor regions (Akin and Zupursky, 2020; Blankenship and Feller, 2010; Kirkby et al., 2013). In contrast with these sensorimotor systems, the MB and many higher-order brain regions are not topographically organized, and neighboring neurons do not respond to similar stimulus features. Instead, connectivity between KCs and their presynaptic partners is stochastic, and sensory-evoked responses are sparse and unpatterned (Caron et al., 2013). We propose that transient unpatterned activity in young animals is a necessary precursor to the unordered and spatially distributed sensory-evoked responses seen in adults, providing a substrate for subsequent adult experiences.

We describe age-dependent spontaneous activity that is restricted to a single cell type within the learning circuit, the α'/β' KCs. Although multi-parallel and distributed processing in MB circuit modules gives rise to associative learning (Aso et al., 2014), the precise role of α'/β' KCs in learned behavior remains less well understood than other MB cell types. Sparse activity in α'/β' KCs may encode sensory information and information about reward or punishment (Krashes et al., 2007; Turner et al., 2008). Behaviorally, α'/β' KCs are required for the acquisition and consolidation of appetitive and aversive olfactory and gustatory associative memories (Krashes et al., 2007; Masek et al., 2015). Because KC activity coincident with salient stimuli are key elements to form associative memories (Vasmer et al., 2014), the poor learning performance of young animals and of older animals manipulated to aberrantly retain high levels of α'/β' KC activity is unexpected. Our results suggest that high α'/β' KC activity is a necessary feature of immature circuits but may acutely interfere with robust learning. Activity state transitions in young animals may refine responses to conditioned stimuli in mature animals. Whether high α'/β' KC activity in young animals organizes or is permissive for the subsequent role of α'/β' KCs in memory acquisition and consolidation remains to be investigated.

Among the MB cell types, only α'/β' KCs undergo a high- to low-activity state transition. α'/β' KCs are not uniquely able to directly transduce JH, because the JH receptors Met and Gce

are highly expressed throughout the MB (Baumann et al., 2017). Cac voltage-gated calcium channels are also highly expressed in the entire MB (Gratz et al., 2019). Nevertheless, α'/β' KCs were found to have the lowest firing threshold and, correspondingly, the highest rate of baseline and odor sensory-evoked spiking of the three KC classes (Inada et al., 2017; Turner et al., 2008). Although these physiological properties were not studied in the context of age, our studies reveal a change in baseline activity states in the first week of adulthood. We therefore speculate that α'/β' KCs are intrinsically more excitable due to a unique gene expression profile (Croset et al., 2018; Davie et al., 2018). Specific ligand- or voltage-gated ion channels or ion pumps may display α'/β' KC-biased expression and may undergo changes in expression in early adulthood that directly contribute to cellular excitability. α'/β' KCs may have distinct plasticity rules that derive from these age-dependent gene expression and excitability changes.

Hormone signaling regulates α'/β' KC physiology with age. Although Cac channels mediate young α'/β' KC spontaneous activity and JH signaling controls the neural activity state transition, a direct JH-to-Cac channel connection is unlikely. We found that Cac mRNA expression in α'/β' KCs does not change over the first week of adulthood (RNA sequencing [RNA-seq] data not shown), consistent with the absence of evidence that Met and Gce hormone receptors directly target Cac channels. We therefore hypothesize that JH may indirectly influence Cac channel function. Our finding that the high activity retained in α'/β' KCs in mature flies with Met and Gce receptors knocked down was sensitive to the voltage-gated calcium channel antagonist PLTX (Figures 3B and S3J) supports an indirect link between JH and these channels. Thus, we speculate that JH signaling normally produces transcriptional changes in young animals that influence the overall physiology and resting membrane potential of α'/β' KCs. These changes in α'/β' KC membrane potential may then reduce Cac channel opening and calcium flux over the first week of adulthood. Future investigation of how the direct targets of JH signaling ultimately influence the membrane potential and Cac function will provide new insights into the underlying circuit maturation mechanisms.

We find that transient hormonal signaling is critically necessary to impart stable changes in neural activity and learned behavior. JH acting on KCs of young animals coordinates the decrease in spontaneous activity and the maturation of adult learned behavior. When JH signaling is disrupted transiently in α'/β' KCs during a sensitive period in young animals, older animals retain high levels of spontaneous KC activity and poor learned behavior, mimicking the activity and behavior of young animals. Thus, hormone signaling is essential for learning circuits to transition from an immature to a mature state capable of robust learning. The JH receptors Met and Gce, like many hormone receptors, can directly alter transcription (Jindra et al., 2013). Gene expression changes downstream of these hormone receptors likely directly or indirectly modulate ion channels, synapses, and neurotransmission, thereby sculpting learning circuits. We speculate that structural refinement of learning circuits underlies the maturation of learned behavior; therefore, further investigation of hormone-triggered molecular changes affecting neurotransmission may provide new entry points for investigating

these fundamental age-dependent processes. Together, these studies provide insight into the maturation of activity states and learned behaviors and a platform to examine how hormonally evoked cellular changes enhance the acquisition and maintenance of learned associations.

STAR★METHODS

Detailed methods are provided in the online version of this paper and include the following:

- **KEY RESOURCES TABLE**
- **RESOURCE AVAILABILITY**
 - Lead contact
 - Materials availability
 - Data and code availability
- **EXPERIMENTAL MODEL AND SUBJECT DETAILS**
 - Fly stocks
- **METHOD DETAILS**
 - GCaMP imaging methods
 - Pharmacology for calcium imaging
 - CaMPARI imaging methods
 - Behavioral assay flies
 - Aversive taste memory behavioral assay
 - Innate sugar or bitter proboscis extension response (PER) behavioral assays
- **QUANTIFICATION AND STATISTICAL ANALYSIS**
 - Analysis of GCaMP imaging
 - Analysis of CaMPARI imaging
 - Analysis of behavior

SUPPLEMENTAL INFORMATION

Supplemental information can be found online at <https://doi.org/10.1016/j.neuron.2021.04.006>.

ACKNOWLEDGMENTS

We thank B. McCabe for the UAS-PLTX flies, A. Charidge-Chang for the UAS-gtACR1-eYFP flies for behavior, and V. Jayaraman for the UAS-gtACR1-mCherry flies for functional imaging. We are grateful to Marla Feller, Matthew Kayser, Colleen Kirkhart, Karly Ortega, and members of the Scott laboratory for advice and comments on the manuscript. This work was supported by an HHMI Early Career Investigator Award (to K.S.), a Jane Coffin Childs Memorial Fund for Medical Research Postdoctoral Fellowship (to S.G.L.), and NIH K99 Award (K99DC018779 to S.G.L.).

AUTHOR CONTRIBUTIONS

S.G.L. and K.S. conceived and designed the study and wrote the manuscript. S.G.L. performed the experiments and analyzed the data.

DECLARATION OF INTERESTS

The authors declare no competing interests.

Received: February 16, 2021

Revised: March 26, 2021

Accepted: April 7, 2021

Published: April 28, 2021

REFERENCES

- Akin, O., and Zipursky, S.L. (2020). Activity regulates brain development in the fly. *Curr. Opin. Genet. Dev.* 65, 8–13.
- Akin, O., Bajar, B.T., Keles, M.F., Frye, M.A., and Zipursky, S.L. (2019). Cell-type-Specific Patterned Stimulus-Independent Neuronal Activity in the *Drosophila* Visual System during Synapse Formation. *Neuron* 101, 894–904.e5.
- Alyagor, I., Berkun, V., Keren-Shaul, H., Marmor-Kollet, N., David, E., Mayseless, O., Issman-Zecharya, N., Amit, I., and Schuldiner, O. (2018). Combining Developmental and Perturbation-Seq Uncovers Transcriptional Modules Orchestrating Neuronal Remodeling. *Dev. Cell* 47, 38–52.e6.
- Argue, K.J., Yun, A.J., and Neckameyer, W.S. (2013). Early manipulation of juvenile hormone has sexually dimorphic effects on mature adult behavior in *Drosophila melanogaster*. *Horm. Behav.* 64, 589–597.
- Aso, Y., Hattori, D., Yu, Y., Johnston, R.M., Iyer, N.A., Ngo, T.-T.B., Dionne, H., Abbott, L.F., Axel, R., Tanimoto, H., and Rubin, G.M. (2014). The neuronal architecture of the mushroom body provides a logic for associative learning. *eLife* 3, e04577.
- Baumann, A.A., Texada, M.J., Chen, H.M., Etheredge, J.N., Miller, D.L., Picard, S., Warner, R., Truman, J.W., and Riddiford, L.M. (2017). Genetic tools to study juvenile hormone action in *Drosophila*. *Sci. Rep.* 7, 2132.
- Ben-Ari, Y., Cherubini, E., Corradetti, R., and Gaiarsa, J.L. (1989). Giant synaptic potentials in immature rat CA3 hippocampal neurones. *J. Physiol.* 416, 303–325.
- Bilen, J., Atallah, J., Azanchi, R., Levine, J.D., and Riddiford, L.M. (2013). Regulation of onset of female mating and sex pheromone production by juvenile hormone in *Drosophila melanogaster*. *Proc. Natl. Acad. Sci. USA* 110, 18321–18326.
- Bischof, J., Björklund, M., Furger, E., Schertel, C., Taipale, J., and Basler, K. (2013). A versatile platform for creating a comprehensive UAS-ORFeome library in *Drosophila*. *Development* 140, 2434–2442.
- Blankenship, A.G., and Feller, M.B. (2010). Mechanisms underlying spontaneous patterned activity in developing neural circuits. *Nat. Rev. Neurosci.* 11, 18–29.
- Bownes, M., and Rembold, H. (1987). The titre of juvenile hormone during the pupal and adult stages of the life cycle of *Drosophila melanogaster*. *Eur. J. Biochem.* 164, 709–712.
- Caron, S.J.C., Ruta, V., Abbott, L.F., and Axel, R. (2013). Random convergence of olfactory inputs in the *Drosophila* mushroom body. *Nature* 497, 113–117.
- Choi, B.J., Imlach, W.L., Jiao, W., Wolfram, V., Wu, Y., Grbic, M., Cela, C., Baines, R.A., Nitabach, M.N., and McCabe, B.D. (2014). Miniature neurotransmission regulates *Drosophila* synaptic structural maturation. *Neuron* 82, 618–634.
- Croset, V., Treiber, C.D., and Waddell, S. (2018). Cellular diversity in the *Drosophila* midbrain revealed by single-cell transcriptomics. *eLife* 7, e34550.
- Davie, K., Janssens, J., Koldere, D., De Waegeneer, M., Pech, U., Kreft, L., Aibar, S., Makhzami, S., Christiaens, V., Bravo González-Blas, C., et al. (2018). A Single-Cell Transcriptome Atlas of the Aging *Drosophila* Brain. *Cell* 174, 982–998.e20.
- Dubnau, J., Grady, L., Kitamoto, T., and Tully, T. (2001). Disruption of neurotransmission in *Drosophila* mushroom body blocks retrieval but not acquisition of memory. *Nature* 411, 476–480.
- Farooq, U., and Dragoi, G. (2019). Emergence of preconfigured and plastic time-compressed sequences in early postnatal development. *Science* 363, 168–173.
- Fisher, Y.E., Yang, H.H., Isaacman-Beck, J., Xie, M., Gohl, D.M., and Clandinin, T.R. (2017). FlpStop, a tool for conditional gene control in *Drosophila*. *eLife* 6, e22279.
- Flatt, T., Moroz, L.L., Tatar, M., and Heyland, A. (2006). Comparing thyroid and insect hormone signaling. *Integr. Comp. Biol.* 46, 777–794.

- Fosque, B.F., Sun, Y., Dana, H., Yang, C.-T., Ohshima, T., Tadross, M.R., Patel, R., Zlatić, M., Kim, D.S., Ahrens, M.B., et al. (2015). Neural circuits. Labeling of active neural circuits in vivo with designed calcium integrators. *Science* 347, 755–760.
- Foster, J.A., and Burman, M.A. (2010). Evidence for hippocampus-dependent contextual learning at postnatal day 17 in the rat. *Learning & Memory* 17, 259–266, <https://doi.org/10.1101/Im.1755810>.
- Gazivova, I., Bonnette, P.C., Henrich, V.C., and Jindra, M. (2004). Cell-autonomous roles of the ecdysoneless gene in *Drosophila* development and oogenesis. *Development* 131, 2715–2725.
- Gratz, S.J., Goel, P., Bruckner, J.J., Hernandez, R.X., Khateeb, K., Macleod, G.T., Dickman, D., and O'Connor-Giles, K.M. (2019). Endogenous tagging reveals differential regulation of Ca²⁺ channels at single active zones during presynaptic homeostatic potentiation and depression. *J. Neurosci.* 39, 2416–2429.
- Gu, H., Jiang, S.A., Campusano, J.M., Iniguez, J., Su, H., Hoang, A.A., Lavian, M., Sun, X., and O'Dowd, D.K. (2009). Cav2-type calcium channels encoded by *cac* regulate AP-independent neurotransmitter release at cholinergic synapses in adult *Drosophila* brain. *J. Neurophysiol.* 101, 42–53.
- Harris, K.M., and Teyler, T.J. (1984). Developmental onset of long-term potentiation in area CA1 of the rat hippocampus. *J. Physiol.* 346, 27–48.
- Harris, D.T., Kallman, B.R., Mullaney, B.C., and Scott, K. (2015). Representations of Taste Modality in the *Drosophila* Brain. *Neuron* 86, 1449–1460.
- Inada, K., Tsuchimoto, Y., and Kazama, H. (2017). Origins of Cell-Type-Specific Olfactory Processing in the *Drosophila* Mushroom Body Circuit. *Neuron* 95, 357–367.e4.
- Jiang, S.A., Campusano, J.M., Su, H., and O'Dowd, D.K. (2005). *Drosophila* mushroom body Kenyon cells generate spontaneous calcium transients mediated by PLTX-sensitive calcium channels. *J. Neurophysiol.* 94, 491–500.
- Jindra, M., Palli, S.R., and Riddiford, L.M. (2013). The juvenile hormone signaling pathway in insect development. *Annu. Rev. Entomol.* 58, 181–204.
- Jindra, M., Uhlirova, M., Charles, J.-P., Smykal, V., and Hill, R.J. (2015). Genetic Evidence for Function of the bHLH-PAS Protein Gce/Met As a Juvenile Hormone Receptor. *PLoS Genet.* 11, e1005394.
- Joëls, M. (1997). Steroid hormones and excitability in the mammalian brain. *Frontiers in Neuroendocrinology* 18, 2–48, <https://doi.org/10.1006/frne.1996.0144>.
- Keene, A.C., and Masek, P. (2012). Optogenetic induction of aversive taste memory. *Neuroscience* 222, 173–180.
- Kirkby, L.A., Sack, G.S., Firl, A., and Feller, M.B. (2013). A role for correlated spontaneous activity in the assembly of neural circuits. *Neuron* 80, 1129–1144.
- Kirkhart, C., and Scott, K. (2015). Gustatory learning and processing in the *Drosophila* mushroom bodies. *J. Neurosci.* 35, 5950–5958.
- Krashes, M.J., Keene, A.C., Leung, B., Armstrong, J.D., and Waddell, S. (2007). Sequential use of mushroom body neuron subsets during *Drosophila* odor memory processing. *Neuron* 53, 103–115.
- Lark, A., Kitamoto, T., and Martin, J.-R. (2017). Modulation of neuronal activity in the *Drosophila* mushroom body by DopEcR, a unique dual receptor for ecdysone and dopamine. *Biochim. Biophys. Acta Mol. Cell Res.* 1864, 1578–1588.
- Lee, T., Lee, A., and Luo, L. (1999). Development of the *Drosophila* mushroom bodies: sequential generation of three distinct types of neurons from a neuroblast. *Development* 126, 4065–4076.
- Lee, T., Marticke, S., Sung, C., Robinow, S., and Luo, L. (2000). Cell-autonomous requirement of the USP/EcR-B ecdysone receptor for mushroom body neuronal remodeling in *Drosophila*. *Neuron* 28, 807–818.
- Lin, H.-H., Cao, D.-S., Sethi, S., Zeng, Z., Chin, J.S.R., Chakraborty, T.S., Shepherd, A.K., Nguyen, C.A., Yew, J.Y., Su, C.-Y., and Wang, J.W. (2016). Hormonal Modulation of Pheromone Detection Enhances Male Courtship Success. *Neuron* 90, 1272–1285.
- Liu, Q., Yang, X., Tian, J., Gao, Z., Wang, M., Li, Y., and Guo, A. (2016). Gap junction networks in mushroom bodies participate in visual learning and memory in *Drosophila*. *eLife* 5, e13238.
- Marchetti, G., and Tavosanis, G. (2017). Steroid Hormone Ecdysone Signaling Specifies Mushroom Body Neuron Sequential Fate via Chinmo. *Curr. Biol.* 27, 3017–3024.e4.
- Masek, P., and Scott, K. (2010). Limited taste discrimination in *Drosophila*. *Proc. Natl. Acad. Sci. USA* 107, 14833–14838.
- Masek, P., Worden, K., Aso, Y., Rubin, G.M., and Keene, A.C. (2015). A dopamine-modulated neural circuit regulating aversive taste memory in *Drosophila*. *Curr. Biol.* 25, 1535–1541.
- McGuire, S.E., Le, P.T., and Davis, R.L. (2001). The role of *Drosophila* mushroom body signaling in olfactory memory. *Science* 293, 1330–1333.
- McGuire, S.E., Le, P.T., Osborn, A.J., Matsumoto, K., and Davis, R.L. (2003). Spatiotemporal rescue of memory dysfunction in *Drosophila*. *Science* 302, 1765–1768.
- Miura, K., Oda, M., Makita, S., and Chinzei, Y. (2005). Characterization of the *Drosophila* Methoprene-tolerant gene product. Juvenile hormone binding and ligand-dependent gene regulation. *FEBS J.* 272, 1169–1178.
- Mohammad, F., Stewart, J.C., Ott, S., Chlebikova, K., Chua, J.Y., Koh, T.-W., Ho, J., and Claridge-Chang, A. (2017). Optogenetic inhibition of behavior with anion channelrhodopsins. *Nat. Methods* 14, 271–274.
- Morsink, M.C., Steenbergen, P.J., Vos, J.B., Karst, H., Joëls, M., De Kloet, E.R., and Datson, N.A. (2006). Acute activation of hippocampal glucocorticoid receptors results in different waves of gene expression throughout time. *J. Neuroendocrinol.* 18, 239–252.
- Murmu, M.S., Stinnakre, J., and Martin, J.-R. (2010). Presynaptic Ca²⁺ stores contribute to odor-induced responses in *Drosophila* olfactory receptor neurons. *J. Exp. Biol.* 213, 4163–4173.
- Nunez, J., Celi, F.S., Ng, L., and Forrest, D. (2008). Multigenic control of thyroid hormone functions in the nervous system. *Mol. Cell. Endocrinol.* 287, 1–12.
- Pascual, A., and Pr  at, T. (2001). Localization of long-term memory within the *Drosophila* mushroom body. *Science* 294, 1115–1117.
- Piekarski, D.J., Boivin, J.R., and Wilbrecht, L. (2017). Ovarian Hormones Organize the Maturation of Inhibitory Neurotransmission in the Frontal Cortex at Puberty Onset in Female Mice. *Curr. Biol.* 27, 1735–1745.e3.
- Rivas, M., and Naranjo, J.R. (2007). Thyroid hormones, learning and memory. *Genes Brain Behav.* 6 (Suppl 1), 40–44.
- Rosay, P., Armstrong, J.D., Wang, Z., and Kaiser, K. (2001). Synchronized neural activity in the *Drosophila* memory centers and its modulation by amnesia. *Neuron* 30, 759–770.
- Takemura, S.-Y., Aso, Y., Hige, T., Wong, A., Lu, Z., Xu, C.-S., Rivlin, P.K., Hess, H., Zhao, T., Parag, T., et al. (2017). A connectome of a learning and memory center in the adult *Drosophila* brain. *eLife* 6, e26975.
- Turner, G.C., Bazhenov, M., and Laurent, G. (2008). Olfactory representations by *Drosophila* mushroom body neurons. *J. Neurophysiol.* 99, 734–746.
- Tuthill, J.C., and Wilson, R.I. (2016). Parallel Transformation of Tactile Signals in Central Circuits of *Drosophila*. *Cell* 164, 1046–1059.
- Vasmer, D., Pooryasin, A., Riemensperger, T., and Fiala, A. (2014). Induction of aversive learning through thermogenetic activation of Kenyon cell ensembles in *Drosophila*. *Front. Behav. Neurosci.* 8, 174.
- Wang, Z., Singhvi, A., Kong, P., and Scott, K. (2004). Taste representations in the *Drosophila* brain. *Cell* 117, 981–991.
- Wilson, T.G., and Fabian, J. (1986). A *Drosophila melanogaster* mutant resistant to a chemical analog of juvenile hormone. *Dev. Biol.* 118, 190–201.
- Wu, M., Manoli, D., Fraser, E., Coats, J., Tollkuhn, J., Honda, S.-I., Harada, N., and Shah, N. (2009). Estrogen masculinizes neural pathways and sex-specific behaviors. *Cell* 139, 61–72, <https://doi.org/10.1016/j.cell.2009.07.036>.
- Xu, C., Luo, J., He, L., Montell, C., and Perrimon, N. (2017). Oxidative stress induces stem cell proliferation via TRPA1/RyR-mediated Ca²⁺ signaling in the *Drosophila* midgut. *eLife* 6, e22441.

Yamanaka, N., Marqués, G., and O'Connor, M.B. (2015). Vesicle-Mediated Steroid Hormone Secretion in *Drosophila melanogaster*. *Cell* **163**, 907–919.

Zhang, X., and Gaudry, Q. (2018). Examining Monosynaptic Connections in *Drosophila* Using Tetrodotoxin Resistant Sodium Channels. *J. Vis. Exp.* **2018**, 57052.

Zhang, S.X., Glantz, E.H., Rogulja, D., and Crickmore, M.A. (2019). Hormonal control of motivational circuitry orchestrates the transition to sexuality in *Drosophila*. *bioRxiv*. <https://doi.org/10.1101/852335>.

Zhou, M., Chen, N., Tian, J., Zeng, J., Zhang, Y., Zhang, X., Guo, J., Sun, J., Li, Y., Guo, A., and Li, Y. (2019). Suppression of GABAergic neurons through D2-like receptor secures efficient conditioning in *Drosophila* aversive olfactory learning. *Proc. Natl. Acad. Sci. USA* **116**, 5118–5125.

STAR★METHODS

KEY RESOURCES TABLE

REAGENT or RESOURCE	SOURCE	IDENTIFIER
Chemicals, peptides, and recombinant proteins		
All-trans retinal	Sigma	Cat#R2500
Tetrodotoxin (TTX)	Tocris	Cat#1078
Ethylene glycol-bis(2-aminoethylether)- <i>N,N,N',N'</i> -tetraacetic acid (EGTA)	Sigma	Cat#E3889
Plectreureys toxin (PLTX)	Alomone labs	Cat#P510
Thapsigargin	Sigma	Cat#T9033
2-octanol	Sigma	Cat#74858
Precocene I	Sigma	Cat#195855
Experimental models: Organisms/strains		
<i>Drosophila</i> : w ⁺ ; UAS-GCaMP6s/+; UAS-GCaMP6s/+; OK107-Gal4/+	Bloomington Drosophila Stock Center	Derived from BDSC_854
<i>Drosophila</i> : w ⁺ ; UAS-GCaMP6s/+; UAS-GCaMP6s/H24-Gal4	Bloomington Drosophila Stock Center	Derived from BDSC_51632
<i>Drosophila</i> : w ⁺ ; UAS-CaMPARI/+; +; OK107-Gal4/+	Bloomington Drosophila Stock Center	Derived from BDSC_58761 and BDSC_854
<i>Drosophila</i> : w ⁺ ; UAS-GCaMP6s/MB008B-AD; UAS-GCaMP6s/MB008B-DBD	Bloomington Drosophila Stock Center	Derived from BDSC_68291
<i>Drosophila</i> : w ⁺ ; UAS-PLTX/UAS-GCaMP6s; UAS-PLTX/UAS-GCaMP6s; OK107-Gal4/+	Choi et al., 2014	N/A
<i>Drosophila</i> : cac ^{MI02836-FlipStop.ND/Y} ; UAS-GCaMP6s/+; tub-GAL80 ^{ts} /UAS-FLPD5; OK107-Gal4/+	Bloomington Drosophila Stock Center	Derived from BDSC_55805, BDSC_854, and BDSC_67681
<i>Drosophila</i> : cac ^{MI02836-FlipStop.ND/Y} ; UAS-GCaMP6s/+; tub-GAL80 ^{ts} /+; OK107-Gal4/+	Bloomington Drosophila Stock Center	Derived from BDSC_67681 and BDSC_854
<i>Drosophila</i> : cac ^{MI02836-FlipStop.ND/Y} ; LexAop-GCaMP6s/UAS-FLPL; MB247-lexA/VT30604-Gal4	Bloomington Drosophila Stock Center	Derived from BDSC_67681 and BDSC_BL62141
<i>Drosophila</i> : cac ^{MI02836-FlipStop.ND/Y} ; LexAop-GCaMP6s/CyO; MB247-lexA/VT30604-Gal4	Bloomington Drosophila Stock Center	Derived from BDSC_67681
<i>Drosophila</i> : w ⁺ ; LexAop-GCaMP6s/+; MB247-lexA, VT30604-Gal4/+	Vienna Drosophila Resource Center and Bloomington Drosophila Stock Center	Derived from VDRC_100638
<i>Drosophila</i> : w ⁺ ; LexAop-GCaMP6s/UAS-Met-RNAi, UAS-Gce-RNAi; MB247-lexA, VT30604-Gal4/+	Vienna Drosophila Resource Center and Bloomington Drosophila Stock Center	Derived from VDRC_100638 and BDSC_61852
<i>Drosophila</i> : w ⁺ ; UAS-CaMPARI/UAS-Met-RNAi, UAS-Gce-RNAi; +; OK107-Gal4/+	Vienna Drosophila Resource Center and Bloomington Drosophila Stock Center	Derived from VDRC_100638, BDSC_61852, BDSC_58761, and BDSC_854
<i>Drosophila</i> : w ⁺ ; UAS-GCaMP6s/+; UAS-GCaMP6s/tub-GAL80 ^{ts} ; OK107-Gal4/+	Bloomington Drosophila Stock Center	Derived from BDSC_854
<i>Drosophila</i> : w ⁺ ; UAS-GCaMP6s/UAS-Met-RNAi, UAS-Gce-RNAi; UAS-GCaMP6s/tub-GAL80 ^{ts} ; OK107-Gal4/+	Vienna Drosophila Resource Center and Bloomington Drosophila Stock Center	Derived from VDRC_100638, BDSC_61852, and BDSC_854
<i>Drosophila</i> : CantonS	N/A	N/A
<i>Drosophila</i> : w ⁺ ; +; VT30604-Gal4/UAS-gtACR1	Vienna Drosophila Resource Center and Mohammad et al., 2017	Derived from VDRC_200228
<i>Drosophila</i> : w ⁺ ; MB005B-AD/+; MB005B-DBD/UAS-gtACR1	Bloomington Drosophila Stock Center and Mohammad et al., 2017	Derived from BDSC_68306
<i>Drosophila</i> : w ⁺ ; +; UAS-gtACR1(attP2)/+	Mohammad et al., 2017	N/A

(Continued on next page)

Continued

REAGENT or RESOURCE	SOURCE	IDENTIFIER
<i>Drosophila</i> : w [*] ; +; UAS-gtACR1(attP2)/+; OK107-Gal4/+	Bloomington <i>Drosophila</i> Stock Center and Mohammad et al., 2017	Derived from BDSC_854
<i>Drosophila</i> : w [*] ; c739-Gal4/+; UAS-gtACR1(attP2)/+	Bloomington <i>Drosophila</i> Stock Center and Mohammad et al., 2017	Derived from BDSC_7362
<i>Drosophila</i> : w [*] ; MB008B-AD/+; MB008B-DBD/UAS-gtACR1	Bloomington <i>Drosophila</i> Stock Center and Mohammad et al., 2017	Derived from BDSC_68291
<i>Drosophila</i> : w [*] ; +; VT44966-Gal4/UAS-gtACR1	Vienna <i>Drosophila</i> Resource Center and Mohammad et al., 2017	Derived from VDRC_203571
<i>Drosophila</i> : w [*] ; +; H24-Gal4/UAS-gtACR1	Bloomington <i>Drosophila</i> Stock Center and Mohammad et al., 2017	Derived from BDSC_51632
<i>Drosophila</i> : w [*] ; +; VT30604-Gal4/+	Vienna <i>Drosophila</i> Resource Center	VDRC_200228
<i>Drosophila</i> : w [*] ; UAS-Met-RNAi, UAS-Gce-RNAi/+; +	Vienna <i>Drosophila</i> Resource Center and Bloomington <i>Drosophila</i> Stock Center	Derived from VDRC_100638 and BDSC_61852
<i>Drosophila</i> : w [*] ; UAS-Met-RNAi, UAS-Gce-RNAi/+; VT30604-Gal4/+	Vienna <i>Drosophila</i> Resource Center and Bloomington <i>Drosophila</i> Stock Center	Derived from VDRC_100638, VDRC_200228, and BDSC_61852
<i>Drosophila</i> : w [*] ; UAS-Met-RNAi, UAS-Gce-RNAi/+; tub-GAL80 ^{ts} /+	Vienna <i>Drosophila</i> Resource Center and Bloomington <i>Drosophila</i> Stock Center	Derived from VDRC_100638 and BDSC_61852
<i>Drosophila</i> : w [*] ; UAS-Met-RNAi, UAS-Gce-RNAi/+; VT30604-Gal4/tub-GAL80 ^{ts}	Vienna <i>Drosophila</i> Resource Center and Bloomington <i>Drosophila</i> Stock Center	Derived from VDRC_100638, VDRC_200228, and BDSC_61852
<i>Drosophila</i> : w [*] ; UAS-GCaMP6s/UAS-gtACR1-mCherry(su(Hw)attP5); UAS-GCaMP6s/+; OK107-Gal4/+	Vivek Jayaraman and Bloomington <i>Drosophila</i> Stock Center	Derived from BDSC_854
<i>Drosophila</i> : w [*] ; UAS-GCaMP6s/+; UAS-dcr2/+; OK107-Gal4/+	Bloomington <i>Drosophila</i> Stock Center	Derived from BDSC_854
<i>Drosophila</i> : w [*] ; UAS-GCaMP6s/+; UAS-dcr2/UAS-ltr-RNAi; OK107-Gal4/+	Vienna <i>Drosophila</i> Resource Center and Bloomington <i>Drosophila</i> Stock Center	Derived from VDRC_6484 and BDSC_854
<i>Drosophila</i> : w [*] ; UAS-GCaMP6s/+; UAS-dcr2/UAS-RyR-RNAi; OK107-Gal4/+	Bloomington <i>Drosophila</i> Stock Center	Derived from BDSC_29445 and BDSC_854
<i>Drosophila</i> : w [*] ; UAS-GCaMP6s/UAS-Cac-RNAi; UAS-dcr2/+; OK107-Gal4/+	Vienna <i>Drosophila</i> Resource Center and Bloomington <i>Drosophila</i> Stock Center	Derived from VDRC_104168 and BDSC_854
<i>Drosophila</i> : w [*] ; UAS-GCaMP6s/+; UAS-dcr2/UAS-Ca- α 1D-RNAi; OK107-Gal4/+	Bloomington <i>Drosophila</i> Stock Center	Derived from BDSC_33413 and BDSC_854
<i>Drosophila</i> : w [*] ; UAS-GCaMP6s/+; UAS-dcr2/UAS-Ca- β -RNAi; OK107-Gal4/+	Bloomington <i>Drosophila</i> Stock Center	Derived from BDSC_29575 and BDSC_854
<i>Drosophila</i> : w [*] ; UAS-GCaMP6s/+; UAS-dcr2/UAS-Ca- α 1D-RNAi; OK107-Gal4/+	Vienna <i>Drosophila</i> Resource Center	Derived from VDRC_51491
<i>Drosophila</i> : w [*] ; UAS-GCaMP6s/UAS- Ca- β -RNAi; UAS-dcr2/+; OK107-Gal4/+	Vienna <i>Drosophila</i> Resource Center	Derived from VDRC_v102188
<i>Drosophila</i> : w [*] ; UAS-GCaMP6s/tub-GAL80 ^{ts} ; UAS-GCaMP6s/UAS-SERCA-RNAi; OK107-Gal4/+	Bloomington <i>Drosophila</i> Stock Center	Derived from BDSC_44581
<i>Drosophila</i> : w [*] ; UAS-GCaMP6s/+; ecd ^{1ts} ; OK107-Gal4/+	Bloomington <i>Drosophila</i> Stock Center	Derived from BDSC_218
<i>Drosophila</i> : w [*] ; UAS-GCaMP6s/CyO; UAS-GCaMP6s/TM2; OK107-Gal4/cID	Bloomington <i>Drosophila</i> Stock Center	Derived from BDSC_854
<i>Drosophila</i> : w [*] ; UAS-GCaMP6s/UAS-EcR.B1-DN; UAS-GCaMP6s/+; OK107-Gal4/+	Bloomington <i>Drosophila</i> Stock Center	Derived from BDSC_6842
<i>Drosophila</i> : w [*] ; UAS-GCaMP6s/UAS-DopEcR-RNAi; UAS-GCaMP6s/+; OK107-Gal4/+	Vienna <i>Drosophila</i> Resource Center	Derived from VDRC_103494
<i>Drosophila</i> : w [*] ; LexAop-GCaMP6s, UAS-Met-RNAi/MB005B-AD; MB247-lexA/MB005B-DBD	Bloomington <i>Drosophila</i> Stock Center and Vienna <i>Drosophila</i> Resource Center	Derived from VDRC_100638 and BDSC_68306
<i>Drosophila</i> : w [*] ; LexAop-GCaMP6s, UAS-Met-RNAi/+; MB247-lexA/+	Vienna <i>Drosophila</i> Resource Center	Derived from VDRC_100638

(Continued on next page)

Continued

REAGENT or RESOURCE	SOURCE	IDENTIFIER
<i>Drosophila</i> : w [*] ; LexAop-GCaMP6s, UAS-Gce-RNAi /MB005B-AD; MB247-lexA/MB005B-DBD	Bloomington Drosophila Stock Center	Derived from BDSC_61852 and BDSC_68306
<i>Drosophila</i> : w [*] ; LexAop-GCaMP6s, UAS-Gce-RNAi/+; MB247-lexA/+	Bloomington Drosophila Stock Center	Derived from BDSC_61852
<i>Drosophila</i> : Met ¹ /Y; UAS-GCaMP6s/+; UAS-GCaMP6s/+; OK107-Gal4/+	Bloomington Drosophila Stock Center	Derived from BDSC_3472
<i>Drosophila</i> : w [*] ; UAS-GCaMP6s/+; UAS-GCaMP6s/UAS-Met.ORF; OK107-Gal4/+	Zurich ORFeome Project	Derived from FlyORF_F000644
<i>Drosophila</i> : w [*] ; UAS-GCaMP6s/MB005B-AD; UAS-GCaMP6s/MB005B-DBD	Bloomington Drosophila Stock Center	Derived from BDSC_68306
Software and algorithms		
MATLAB R2016b	The MathWorks	https://www.mathworks.com/products/matlab.html
SlideBook	3i Intelligent Imaging Innovations	https://www.intelligent-imaging.com/
FIJI (ImageJ)	National Institutes of Health	https://fiji.sc/
GraphPad Prism 6	GraphPad Software	https://www.graphpad.com/scientific-software/prism/

RESOURCE AVAILABILITY

Lead contact

Further information and requests for resources and reagents may be directed to and will be fulfilled by the Lead Contact, Dr. Kristin Scott (kscott@berkeley.edu).

Materials availability

Fly strains generated in this study are available from the Lead Contact upon request.

Data and code availability

All relevant data supporting the findings of this study and code used for analyses are available from the Lead Contact upon request.

EXPERIMENTAL MODEL AND SUBJECT DETAILS

Fly stocks

Drosophila stocks were maintained on standard cornmeal, agar and molasses food at 25 degrees, except as noted below. Full genotypes listed in [Table S1](#).

METHOD DETAILS

GCaMP imaging methods

Calcium transients were imaged in flies expressing GCaMP6s. Male flies of the indicated ages (in days post-eclosion) were used unless otherwise noted. When female flies were used, they were group housed with males and mated. All experiments were performed *in vivo* except as noted. Briefly, for *in vivo* preparations, flies were quickly anesthetized, mounted into custom chambers and the proboscis was waxed in an extended position ([Harris et al., 2015](#)). Ice cold artificial hemolymph solution (AHL) was applied to the head, a window in the head cuticle was dissected and air sacs were removed to allow visualization of the mushroom body. For *ex vivo* experiments, brains were dissected out of flies of the appropriate age in ice cold AHL solution. Brains were then placed on a charged glass slide in a small drop of cold AHL solution. All functional imaging was performed on a fixed-stage 3i spinning disk confocal microscope with a piezo drive and a 20x water objective (1.6x optical zoom) ([Harris et al., 2015](#)). A volume encompassing a portion of the mushroom body was imaged at 0.44 or 1.2 Hz.

Pharmacology for calcium imaging

- Tetrodotoxin (TTX, Tocris 1078): 1 μ M with a 10 min pre-incubation period prior to imaging. This TTX concentration blocks *Drosophila* synaptic transmission ([Rosay et al., 2001](#); [Tuthill and Wilson, 2016](#); [Zhang and Gaudry, 2018](#); [Zhou et al., 2019](#)).
- EGTA (Sigma E3889): 2 mM in calcium chloride-free AHL solution.
- Plectreurys toxin (PLTX, Alomone labs P510): 100 nM with a 15 min pre-incubation period prior to imaging.

- (D) Thapsigargin (Sigma T9033): 20 μ M with a 15 min pre-incubation period prior to imaging.
- (E) 2-octanol (Sigma 74858): 10 mM with a 10 min pre-incubation period prior to imaging.
- (F) Precocene I (Sigma 195855): 10 μ L of 0.1% v/v solution in ethanol applied to the surface of a fly food vial (or ethanol solvent control), dried 1 hour and then newly eclosed flies were added (Lin et al., 2016). Flies were flipped to freshly prepared Precocene vials every 48 hours until imaging.

CaMPARI imaging methods

Male flies of the indicated ages (in days post-eclosion) expressing UAS-CaMPARI in all Kenyon cells were prepared for *in vivo* imaging as described above for GCaMP calcium imaging. A focal plane containing the mushroom body lobes was visualized using the 488 nm laser on a 3i spinning disk confocal microscope. An X-Cite light source with the UV-DAPI filter was then applied for five seconds to induce photoconversion of the active Kenyon cells. Three minutes after the UV photoconversion, the lobes of the mushroom bodies were scanned with a 561nm and a 488 nm laser. (Mock control experiments without UV light showed that imaging the mushroom body z stack with these 561nm and 488 nm laser parameters alone did not induce any photoconversion.).

Behavioral assay flies

Flies for behavioral experiments were raised at 25 unless otherwise noted and young day 1 mated female flies or mature day 7-8 mated female flies were tested.

Aversive taste memory behavioral assay

Newly eclosed virgins were transferred in groups (20-25 females, 6-8 males) to new vials and aged for the indicated number of days. Flies were starved at room temperature for 22-26 hours prior to the experiment in vials with two kimwipes soaked in 5 mL of H₂O. Female flies were then mounted with nail polish on glass slides with brief CO₂ anesthesia (10-18 flies per slide) and then allowed to recover in a humid box for 2-3 hours prior to the experiment. At the start of the experiment all flies were allowed to drink water until satiation. (1) Pre-testing: Flies were then presented with a 200 mM sucrose conditioned stimulus (CS, Sigma) on the legs for three trials before pairing. (2) Training: CS presentation was then paired with the bitter unconditioned stimulus (US) of 50 mM quinine (Sigma) on the proboscis three times (2 minute inter-trial interval). Any fly that did not extend its proboscis for all three sucrose pre-trials and for the first pairing was removed from the study. During the second and third pairings, the US was only presented when flies performed a PER in response to the CS. (3) Testing: Learning was then tested by presenting the CS alone for six trials beginning 5 minutes after the final pairing (5 min inter-trial interval). Aversive taste memory performance is independent of post-ingestive feedback (Keene and Masek, 2012). Flies that did not perform a proboscis extension to sucrose, and hence showed successful learned suppression, were counted and compared with the number of flies that did extend (either partially or fully).

For *acute* silencing with ACR1 exclusively during the behavioral assay and *not* during early adult maturation, flies were collected and raised in groups (20-25 females, 6-8 males) and then transferred to retinal food (400 μ M all-trans retinal added to standard fly food) on day 4. Flies were starved on day 6 as described above and then assayed 23-25 hours later on day 7. Flies were kept in the dark from eclosion until the start of the assay (including during the starvation and the post-mounting recovery period). A green laser (532 nm, LaserGlow LBS-532) was used to acutely silence the ACR1 expressing Kenyon cells or genetic controls. The green laser was focused on individual flies, turned on 30 s prior to the first pre-test and kept focused on the fly for the duration of the assay, until after the 5 min post-final pairing sucrose test.

For silencing experiments using ACR1 during early adult maturation, but *not* during the aversive taste memory assay, crosses were set up on retinal food (400 μ M all-trans retinal added to standard fly food) in the dark. Newly eclosed flies were transferred in groups (20-25 females, 6-8 males) to new retinal food vials. For dark only rearing, flies were raised at 25 degrees in vials wrapped with aluminum foil. For early adult maturation (day 0-2) silencing, vials with newly eclosed flies were placed in a box with constant green light exposure from bright LED lights (in a custom Arduino controlled light box) for 48-56 hours at 25 degrees. 2 day old flies from both conditions were transferred to fresh (no retinal) food vials and aged until day 6 or 7, then starved for 22-26 hours, mounted, allowed to recover in the dark and tested as above (with the lowest possible microscope white light setting for the assay duration). For delayed (day 4-7) silencing experiments, flies were instead transferred to the green light box on day 4, then starved on day 6 and maintained in the light box until they were mounted on slides to be assayed 23-25 hours later on day 7.

For *tub-GAL80^{ts}* experiments, flies were raised at 18 degrees until eclosion and then newly eclosed virgins were transferred in groups (20-25 females, 6-8 males) to new vials and reared either (1) at 30 degrees from day 0-2 and then returned to 18 degrees or (2) at 18 degrees until day 4 and then shifted to 30 degrees. Flies were kept at 18 or 30 degrees for the duration of the starvation period and then mounted and tested (as above).

Innate sugar or bitter proboscis extension response (PER) behavioral assays

PER was assayed as previously described (Wang et al., 2004). Briefly, young day 1 or mature day 7-8 CantonS flies were starved 22-26 hours as above and then mounted and allowed to recover for 2-3 hours. Flies were then water satiated and presented with 4 concentrations of sucrose or of a sucrose-bitter mix three times each. Specifically, for innate sucrose PER, flies were presented on their tarsi three times with 5 mM sucrose followed by 40, 200 and 1000 mM sucrose, in order of increasing concentration. For

innate bitter PER, flies were presented on their proboscises three times each with quinine (0.1, 0.5, 5 and 50mM, in increasing concentration order) in a 100mM sucrose solution. Flies extended their proboscis (1) or did not extend (0) and the average of the 3 trials was calculated.

QUANTIFICATION AND STATISTICAL ANALYSIS

All data analysis was performed in MATLAB or Microsoft Excel and statistical tests were performed in GraphPad Prism. All statistical tests, significance levels, number of observations (N) and other relevant information for data comparisons are specified in the respective figure legend.

Analysis of GCaMP imaging

GCaMP images were registered and ROIs drawn in FIJI (ImageJ). A maximum intensity projection encompassing the Z-depth of the mushroom body was registered (rigid body registration) to correct for X-Y motion artifacts and used for analysis. Large ROIs were drawn manually corresponding to the tip of the α' or α vertical lobe. ROIs corresponding to the heel of the β' or β horizontal lobe or the γ lobe were also drawn for experiments in Figure 1. As individual α'/β' and α/β KCs all have bifurcating axons, with one branch projecting in the vertical α' or α lobe and one branch projecting in the horizontal β' or β lobe, the activity in α' or α ROIs was taken to represent that cell-type, as noted for experiments in Figures 2 and 3. In addition, a large ROI was drawn in a region adjacent to the mushroom body that did not express GCaMP to measure background autofluorescence. In some experiments, each hemisphere of the brain of a fly was analyzed independently, as noted in relevant figure legends. Analysis of fluorescence changes over time was performed in MATLAB. Specifically, custom MATLAB scripts were used to subdivide and tile these large ROIs with a grid of small three by three pixel ROIs, representing small clusters of spatially contiguous axons. Mean fluorescence levels from the background ROI were subtracted from the mushroom body ROIs at each time point, resulting in the fluorescence trace over time: $F(t)$. $\Delta F/F$ (%) was measured as follows: $100\% * (F(t) - F(0)) / F(0)$, where $F(0)$ was the average $F(t)$ of all time points excluding the first two. The standard deviation of $\Delta F/F$ was calculated, and the small three by three pixel ROI with the median standard deviation of $\Delta F/F$ was used to represent the activity in a given lobe of a fly. One or two way ANOVA tests with Sidak's multiple comparison correction on the standard deviation of the $\Delta F/F$ were computed in GraphPad Prism software. Standard deviation projection images were also generated in FIJI (ImageJ). To analyze the magnitude of the calcium signal as a function of frequency, the MATLAB Fast Fourier transform (FFT) algorithm was applied to $\Delta F/F$ timeseries traces for ROIs in the α' or α vertical lobe from flies of each age and one-sided power spectrum density estimates were plotted in MATLAB.

Analysis of CaMPARI imaging

CaMPARI images were analyzed with FIJI (ImageJ). Specifically, large ROIs were drawn manually corresponding to the tip of the α' or α vertical lobe, the heel of the β' or β horizontal lobe and a background region adjacent to the mushroom body. Mean fluorescence levels from the background ROI were subtracted from the mushroom body ROIs in the red (561 nm) and green (488 nm) channels. The ratio of red to green signal, which represents the calcium activity during the time period of UV photoconversion, was calculated by dividing the background subtracted red fluorescence value by the background subtracted green value for each ROI. Two-way ANOVA tests with Sidak's multiple comparison correction were performed with GraphPad Prism software.

Analysis of behavior

For aversive taste memory behavioral assays, 95% confidence intervals for proportions were calculated in Microsoft Excel. Fisher's Exact Tests with Benjamini-Hochberg adjusted P values (False discovery rate of 0.05) were used to identify significant differences in the proportion of flies that extended or did not extend their proboscis at the first test 5 minutes after the final pairing. For silencing experiments using ACR1, Fisher's Exact Test with Benjamini-Hochberg adjusted P values (False discovery rate of 0.05) was used to compare dark reared and silenced flies of the same genotype. For innate sugar or bitter proboscis extension response (PER) assays, young and mature PER fractions were compared with Mann-Whitney U tests.